Analyzing and Reducing DTI Tracking Uncertainty by Combining Deterministic and Stochastic Approaches

Khoa Tan Nguyen, Anders Ynnerman, and Timo Ropinski

Scientific Visualization Group, Linköping University, Sweden
{tan.khoa.nguyen,anders.ynnerman,timo.ropinski}@liu.se

Abstract. Diffusion Tensor Imaging (DTI) in combination with fiber tracking algorithms enables visualization and characterization of white matter structures in the brain. However, the low spatial resolution associated with the inherently low signal-to-noise ratio of DTI has raised concerns regarding the reliability of the obtained fiber bundles. Therefore, recent advancements in fiber tracking algorithms address the accuracy of the reconstructed fibers. In this paper, we propose a novel approach for analyzing and reducing the uncertainty of densely sampled 3D DTI fibers in biological specimens. To achieve this goal, we derive the uncertainty in the reconstructed fiber tracts using different deterministic and stochastic fiber tracking algorithms. Through a unified representation of the derived uncertainty, we generate a new set of reconstructed fiber tracts that has a lower level of uncertainty. We will discuss our approach in detail and present the results we could achieve when applying it to several use cases.

1 Introduction

Diffusion Tensor Imaging (DTI) is a magnetic resonance imaging (MRI) technique that allows non-invasive imaging of the diffusion process of water molecules in biological tissues, such as muscles, or brain white matter. Experimental evidence has shown that the water diffusion in an organized tissue is *anisotropic* [1], as the diffusion magnitude is dependent on the diffusion direction [2]. These characteristics of water diffusion can be mathematically represented by a diffusion tensor field in which the main eigenvector of each tensor corresponds to the direction of the greatest diffusion [3]. By following the main diffusion within a tensor field, a DTI data set can be represented as a set of extracted fiber tracts, or three-dimensional pathways. Alternatively, more advanced techniques based on exploiting the use of probability models or bootstrapping can be used to reconstruct the corresponding three-dimensional pathways. As these tractography algorithms allow for extraction of information regarding connectivity in the brain, they are of great interest to a wide variety of medical and biomedical applications, such as the study of brain development, cerebral ischemia, neurodegenerative diseases [4], and neurosurgical scenarios, such as epilepsy surgery or other cranial surgical interventions. However, despite the potential of DTI, the reliability of the reconstructed fibers is often questioned. This is due to the fact that DTI data are usually of low resolution and suffering from a low signal to noise ratio. Additionally, many sources for uncertainty occur during the long acquisition process as well as the processing and visualization of DTI data. Consequently, the use of DTI fiber tracking in clinical practice is limited, and a more pervasive and reliable use of DTI tractography results can be enabled only by understanding and reducing the involved uncertainty.

In this paper, we propose a novel approach for analyzing and reducing the uncertainty in the context of DTI tractography algorithms. To achieve this goal, we derive the uncertainty information from different sets of reconstruct fibers using different deterministic and stochastic fiber tracking algorithms. The derived uncertainty is then represented in a unified way and serves as the foundation for the generation of a new set of fiber tracts with a lower level of uncertainty. This enables an effective approach to the fusion of different

uncertainty sources, and the application to real-world and synthetic data shows that it yields improved fiber tracking result.

The remainder of the paper is structured as follows. In the next section, we review work related to the proposed approach. In Section 3, we present the derivation and reduction of uncertainty from different fiber tracking algorithms. We then present our visual computing system used to reveal the information of the analysis process in Section 4. We apply the proposed technique to different data set and report the results in Section 5, and conclude the paper in Section 6.

2 Related Work

DTI tractography. DTI fibers tracking [5,6] represents a collection of different algorithms for reconstructing the brain nerve fibers from diffusion-weighted magnetic resonance (MR) data. These algorithms can be roughly classified into two categories: deterministic and stochastic approaches. Deterministic algorithms do initially not associate uncertainty values with the reconstructed trajectory, and all reconstructed trajectories are inherently considered as equally probable. Moreover, deterministic algorithms, without extension, produce only one reconstructed trajectory per seed point, and therefore branching of fascicles will not be represented. However, bootstrapping makes it possible to obtain uncertainty information for the tracking results [7,8]. While conventional bootstrapping requires several scans and introduces additional registration artifacts, it could be shown that the wild bootstrap technique, which works on a single diffusion-weighted data set [9], can achieve comparable reconstruction results [10]. In contrast to deterministic methods, stochastic algorithms incorporate multiple pathways emanating from the seed points and from each point along the reconstructed trajectories. These algorithms, however, are often criticized for making *a-priori* assumptions about the characteristics of uncertainty in the data [11,12]. For instance, when using probability distribution functions (PDFs), it can lead to an ad hoc formulation of relationships between the anisotropy of the diffusion process and the uncertainty of the estimated principal eigenvector of the diffusion tensor [10]. Consequently, the sources of errors are not truly considered, and uncertainty is generally modeled based on a Gaussian formulation. However, when analyzing the uncertainty derived from both, wild bootstrap and probability-based techniques, new fiber tracts with a potentially lower degree of uncertainty can be obtained, and thus the dependency on the *a-priori* assumptions can be reduced.

Deterministic algorithms are based on line propagation algorithms that use local tensor information for each step of the propagation. The FACT (Fiber Assignment by Continuous Tracking) is one of the first streamline tracking techniques in this group [5,13,14]. Another commonly used fiber tracking algorithm is called tensorline [15], and makes use of the full diffusion tensor to deflect the estimated fiber trajectory. There has been two main drawbacks in deterministic tractography. As these algorithms cannot represent branching of fascicles, and provide no indication of the uncertainty, Whitcher et al. proposed the use of the wild bootstrap technique to derive uncertainty from the underlying diffusion-weighted data and then use these results as the foundation for tracking algorithms [9]. While the traditional bootstrap technique provides good estimates of uncertainty in DTI datasets [7,8], it requires multiple scans, which is not an optimal solution in clinical practice. However, Jones has reported that the results from the wild bootstrap approach are comparable to the ones using the traditional bootstrap technique [10]. The main difference between the deterministic and the stochastic approaches is the use of a probability model, which allows to consider multiple pathways emanating from each seed point as well as from each point along the reconstructed trajectories. As a result, one obtains not only the fiber bundles but also the uncertainty associated with the fibers [7,9,11].

DTI Visualization. The reconstructed fiber trajectories can be visualized in several different ways such as glyphs [16,17,18], streamlines, streamtubes [19], and hyperstreamlines [17,20]. To reduce the complexity of

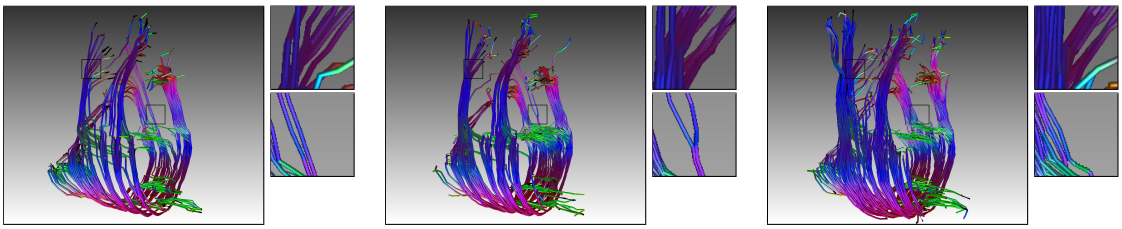

(a) FACT with wild bootstrap (b) Bayesian (c) PICo

Fig. 1. Visualization of fiber bundles reconstructed by using the FACT algorithm with wild bootstrapping (*a*), the Bayesian approach (*b*), and the PICo approach (*c*).

the geometry of the fiber tracts, several techniques have been proposed, such as wrapped streamlines [21], hierarchical principal curves [22], color-mapping [23,24], texture patterning of fiber dissimilarity [25], or topological simplification [26]. Furthermore, various clustering techniques [27] can help to group similar fiber tracts to reduce visual clutter. However, these techniques make it also more difficult to show the uncertainty associated with individual fibers. Lodha et al. [28] proposed a visualization pipeline to reveal the uncertainty in fluid flow which can be applied to the visualization of DTI fibers. Chen et al. proposed a novel interface for exploring densely sampled 3D DTI data [29]. Driven by known embedding methods, the proposed framework provides the ability to project characteristics of fiber tracts from 3D space to a 2D space in such a way that the distance between points are preserved as much as possible. A significant drawback of this approach is the the lack of anatomical interpretation. Besides visualization, the ability for scientists to interactively explore and select DTI fibers for inspection is often desired. However, visual exploration and analysis of densely sampled DTI in 3D is challenging due to the visual clutter caused by the complexity of the geometry. Hence, a substantial amount of research has been focused on solving the difficulties in interacting with densely sampled DTI fibers by proposing new visual forms or novel interaction methods [30]. Sherbondy et al. [31] proposed a set of interaction techniques for exploring the brain connectivity and interpreting pathways. The main operations provided to neuroscientists are the placement and manipulation of box-shaped or ellipsoid-shaped regions in coordination with a simple and flexible query language. Blaas et al. [32] proposed a similar approach for efficient selection of fiber tracts. Jianu et al. [25,33] proposed an interactive approach to navigate through complex fiber tracts in 3D. More recently, Brecheisen et al. proposed a novel framework to visually explore the effect of parameter variation to the reconstructed fiber tracts [34]. The basis for this visualization technique is the pre-computation of all fiber tracts from all possible combination of threshold values and thus provides the user with a better understanding of the tractography result.

3 Uncertainty Derivation and Reduction

In this section, we will introduce how to reduce fiber tracking uncertainty by incorporating three of the most widely used approaches: FACT with wild bootstrapping, the Bayesian approach, and the probability index of connectivity (PICo) approach. However, to be able to perform this desired uncertainty reduction, we need to first derive a common uncertainty measure for these incorporated tractography algorithms.

In a DTI experiment, the diffusion-weighted signal S is modeled by

$$S(g_j) = S_0 \, exp(-b \, g_j^T \, D \, g_j) \quad \text{with } j = 1, 2, \ldots, N \tag{1}$$

where S_0 is the signal intensity with no diffusion gradients applied, b is the diffusion weighting factor, D is an effective self-diffusion tensor in the form of a 3×3 positive define matrix, g is a 3×1 unit vector of the diffusion-sensitive gradient direction, and N is the total number of experiments, including repeated measurements. By applying a log transform, Equation 1 can be structured into the well-known multiple linear regression form [3]:

$$y = X\beta + \varepsilon \tag{2}$$

where $y = \left[ln(S(g_1)), ln(S(g_2)), \ldots, ln(S(g_N))\right]^T$ are the logarithms of the measured signals, $\beta = \left[D_{xx}, D_{yy}, D_{zz}, D_{xy}, D_{xz}, D_{yz}, ln(S_0)\right]^T$ are the unknown regression coefficients consisting of the six unique elements of the self-diffusion tensor, D, $\varepsilon = \left[\varepsilon_0, \varepsilon_1, \ldots, \varepsilon_N\right]^T$ are the error terms, and X is a matrix of different diffusion gradient directions.

$$X = -b \begin{pmatrix} g_{1x}^2 & g_{1y}^2 & g_{1z}^2 & 2g_{1x}g_{1y} & 2g_{1x}g_{1z} & 2g_{1y}g_{1z} & 1 \\ \vdots & \vdots & \vdots & \vdots & \vdots & \vdots & \vdots \\ g_{Nx}^2 & g_{Ny}^2 & g_{Nz}^2 & 2g_{Nx}g_{Ny} & 2g_{Nx}g_{Nz} & 2g_{Ny}g_{Nz} & 1 \end{pmatrix}$$

Based on this mathematical representation, the diffusion tensor can be estimated through the use of weighted least squares (WLS) regression.

Wild Bootstrap Approach. This is a model-based resampling technique, designed to investigate the uncertainty in linear regression with heteroscedasticity, i. e., non-constant variance with different regressors of unknown form [8]. Wild bootstrap resampling is defined as:

$$y_i^* = x_i\hat{\beta} + e_i^* \tag{3}$$

where the resampling error e_i^* is:

$$e_i^* = \frac{y_i - \hat{\mu}_i}{(1-h_i)^{1/2}} t_i \tag{4}$$

Here, t_i are independent and identically distributed (i.i.d) random variables with $E(t_i) = 0$, and $E(t_i^2) = 1$, the leverage value h_i is the i-th diagonal element of the hat matrix defined in the WLS process, and $\hat{\mu}_i$ is the i-th WLS fitted log measurement.

In this technique, a bootstrap sample set $y_i^* = [y_1^*, y_2^*, \ldots, y_N^*]$ undergoes the WLS fitting procedure which leads to D^*, based on which a non-linear DTI parameter $\hat{\theta}^*$ such as fractional anisotropy (FA) is calculated. The repetition of resampling e_i^* and calculating the non-linear parameter $\hat{\theta}^*$ through a fixed large number, N_B, of times (typically from hundreds to thousands of times) will yield the underlying uncertainty from the diffusion data. Particularly the N_B independent bootstrap samples $\hat{\theta}^{*b}$, $b = 1, 2, \ldots, N_B$ represent the replication of $\hat{\theta}$, which is an estimation of the true unknown θ using the original sample y by WLS, with the associated uncertainty e_i^*.

In our approach, we apply an averaging scheme over the resampled e_j^* and use this as the uncertainty at each point along the reconstructed fiber

$$u_{\mathrm{W}} = \frac{\sum_1^{N_B} e_j^*}{N_B}$$

In general, with all incorporated algorithms, we omit the usage of a direction-weighted error computation scheme, as the branching nature of the probability fiber tracts, enables us to obtain this uncertainty in a dense manner around each fiber.

Bayesian Approach. This technique makes use of the local PDF to capture the uncertainty at each voxel of the reconstructed fiber [11]. In particular, it is assumed that there is only one fiber orientation in each voxel, and any deviations from the model will be captured as uncertainty in this orientation. In each voxel, given combination of data and model, the likelihood of the fiber orientation along an axis X is formulated as:

$$P(X|D) = \frac{P(D|X)P(X)}{P(D)} \tag{5}$$

Given the principal direction X, by applying WLS regression to solve the linear regression system described in Equation 2 for a fixed large number of times, N_B, the model yields the predicted measurement $\hat{\mu}_i$, $i = 1,\ldots,N_B$. The observed data, y_i, is a noisy estimate of $\hat{\mu}_i$ which is modeled as:

$$ln(y_i) = ln(\hat{\mu}_i) + \varepsilon_i \tag{6}$$

where ε_i is Gaussian distributed as $N(0, \frac{\sigma^2}{\hat{\mu}_i^2})$, where σ^2 is the variance of the noise contained in the MRI data. As a result, the likelihood of the fiber along the axis X at a voxel is given as:

$$P(D|X) = P(y_1|\hat{\mu}_1)P(y_2|\hat{\mu}_2)\ldots P(y_{N_B}|\hat{\mu}_{N_B}) \tag{7}$$

With the assumption that the prior distribution for all parameters except X is a dirac delta function, $P(D)$ is then the integral of $P(D|X)$ over the sphere. For diffusion tensor data, the priors of S_0 and the tensor eigenvalues are fixed around the maximum-likelihood estimate (MLE). Thus, the function $P(D|X)$ can be evaluated by setting the tensor principal direction to X and computing the likelihood of the observed data.

As shown in Equation 7, one can derive the underlying uncertainty information from the diffusion data and this information reveals the uncertainty associated with each reconstructed fiber. In this work, we apply an averaging scheme on the uncertainty derived from the Monte Carlo random walk process to derive the uncertainty of each point along the reconstructed trajectory

$$u_{\mathrm{b}} = \frac{\sum_{i=1}^{N_B} P(y_i|\mu_i)}{N_B} \tag{8}$$

Probability Index of Connectivity (PICo) Approach. Parker et al. have proposed a novel approach to associate uncertainty with the reconstructed trajectories [12]. This is achieved by relating the probability of a tract with the number of times it is reconstructed in a Monte Carlo random walk, where the characteristics of the random walk are governed by the properties of the diffusion tensor, i. e., fractional anisotropy (FA). The PICo approach incorporates the directional uncertainty into the fiber tracking process at every step along its length by defining a modified principal eigenvector $v_{1mod}(x,n) = v_1'(x) + \delta v_1'(x,n)$, where n indexes the iteration of a Monte Carlo process. Similarly, one can define $v_{1mod}'(x,n) = v_1'(x) + \delta v_1'(x,n)$ within a rotated frame of reference x', y', z', where $v_1'(x)$ is simply $v_1(x)$ rotated into the new frame of reference with z' defined by $v_1(x)$. As a result, $\delta v_1'(x,n)$ is defined by the angles $\delta\theta'(x,n)$ and $\delta\phi'(x,n)$, which are obtained from the PDF of possible fiber bundle orientations at each point encountered during the tracing process.

Two methods have been proposed for calculating the uncertainty in the orientation of the principal diffusion direction v_1: 0^{th} order and 1^{st} order cases. In the 0^{th} order case, the uncertainty in the principal diffusion direction v_1 is defined by the tensor anisotropy, providing an isotropic normal distribution of orientation centered on the original estimate of v_1. A sigmoid function is applied to the standard deviation (SD) of the distribution of possible values for $\delta\theta'(x)$ to link the uncertainty to FA. In the 1^{st} order case, the uncertainty is dependent on the skewness of the tensor through the analysis of the minor eigenvectors, v_2 and v_3, and their corresponding eigenvalues. As a result, this provides a more accurate distribution of orientation

in the case of oblate tensor ellipsoids. Detail information about the choice of proper the PDF are discussed in [12] and [35].

To derive uncertainty, let $\chi(V,N)$ be the number of occasions a voxel V is crossed by the reconstructed trajectories over N repetitions during the fiber tracking process. The map of the probability, Ψ, of connection to the seeding point can be formulated as

$$\Psi(V) \approx \Psi(V,N) = \frac{\chi(V,N)}{N} \tag{9}$$

where Ψ reflects the definition of uncertainty of eigenvector orientation mentioned above. Therefore, in this work we use Ψ to depict the associated uncertainty for points along the reconstructed fibers and refer to it as u_p.

Although the uncertainty values as used in the different tractography algorithms can be traced back to the same data set, the outcome of the tracing stage can vary substantially. Figure 1 shows a comparison of the tractography results of the three discussed algorithms. The closeups on the right of each subfigure emphasize some characteristic differences. To be able to fuse uncertainties from different sources, it must be possible to relate them to each other. Therefore, it is important to note, that although the incorporated uncertainty values are calculated using different schemes, they are all based on the distribution of the FA parameter of the underlying diffusion tensor field. Although the idea of comparing the derived uncertainty from the wild bootstrapping and other Monte Carlos based techniques has been proposed in [36,37], their approach focuses on the numerical analysis of the derived uncertainty and quantitatively assess the reconstructed fibers through visualization. In our approach, we provide the ability to not only compare the derived uncertainty but also allowing the reduction of these values through visual analysis. As a result, these uncertainty values can be used together as a foundation for the uncertainty reduction, as we show in Section 5. To allow a more meaningful relation, all derived uncertainty values are normalized to lie in the interval $[0,1]$.

Uncertainty Reduction. Based on the analysis of the derived uncertainty discussed above, we propose a novel method to generate a new set of fiber tracts that has a lower uncertainty level. In order to achieve this, we first identify matching fiber tracts from different set of reconstructed fibers using different fiber tracking algorithms, e. g. FACT with wild bootstrap, Bayesian tractography, and PICo tractography. We then estimate the intersections between these fiber tracts. As the FACT with wild bootstrap, the Bayesian, and the PICo tractography are based on the line propagation algorithm to track the trajectories, the distance between two consecutive points along a reconstructed fiber depends on the step size used in the fiber tracking process. Moreover, in order to limit the effect of numerical error propagation, a lower bound and a upper bound threshold are pre-defined for the estimation of intersections. Let $d(p_i^k, p_j^l)$ denote the distance between the point p_i on the fiber k and the point p_j on the fiber l. Then, the condition for an intersection is formulated as

$$u \leq d(p_i^k, p_j^l) \leq v \tag{10}$$

where u is the lower bound and v is the upper bound threshold.

Once the intersections have been identified, the fibers are divided into segments. The average uncertainty of each segment is used as the foundation to generate a new fiber tract by combining corresponding segments with lower uncertainty. As a result, this enables us to achieve a new set of fibers with low uncertainty. The advantage of using an averaging scheme is to reduce the *a-priori* assumption in the probabilistic tractography algorithms, e. g. Bayesian and PICo tractography. For instance, depending on the input *a-priori* information, the PDFs in the Bayesian tractography can lead to an ad hoc formulation of relationships between the anisotropy of the diffusion process and the uncertainty of the estimated principal eigenvector of the diffusion tensor [10]. On the other hand, the wild bootstrapping technique does not have this property. Therefore, an

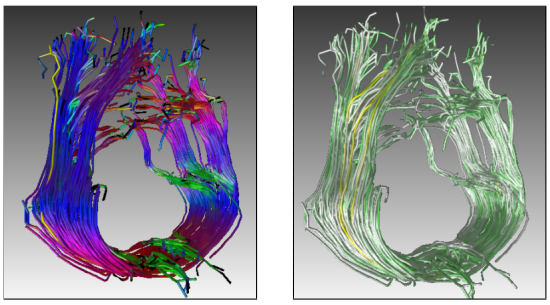

(a) (b)

Fig. 2. Visualization of DTI fibers using the streamtube representation. (*a*) is the visualization of the reconstructed fibers using streamtubes with the color mapped to the normal vector at each point along the fibers. (*b*) is the visualization of the same fibers with the uncertainty mapped to the saturation of the color.

averaging scheme can help to reduce the *a-priori* assumption when fusing the uncertainty from these fiber tracking algorithms. It is worth noting that depending of the application cases or the involvement of domain knowledge the proposed technique can be easily extended to more advanced uncertainty fusion schemes.

4 Interactive System Setup

In order to verify our approach and to influence the proposed fiber reduction, we have developed an interactive visual computing system, which we briefly present in this section.

3D Fibers Visualization. There have been many visual representations proposed for visualizing fibers in the last years [16,17,19,20,38,39]. Although the streamline representation has the advantage of being a fast method due to its low geometry complexity, lines with more than one pixel suffer from gaps in highly curved areas. In addition, depth perception is not supported when lines with a constant density are used [19]. On the other hand, streamtubes provide better depth cues as they allow a shaded surface visualization, which helps to improve the perception of the fibers' structure [19]. As a result, we make use of the streamtube representation in our system, to be able to represent the set of reconstructed fibers together with their uncertainty expressed through color saturation.

It is worth noting that the rendering of streamtubes are more demanding due to its complex geometry structure. In order to achieve high quality visualization, we exploit the use of vertex buffer objects (VBOs) to accelerate the visualization of densely sampled DTI fibers. For instance, we separate the geometry description of the fibers and their associated parameters, e. g. FA, MD, and uncertainty values. These values are stored in textures, which are associated with the fibers through texture coordinates. This enables us to map multiple values of interest into different visual representations to provide not only high quality visualization but also at an interactive frame rates, which is essential to explore the derived uncertainties. Figure 2 illustrates the visualization of the same reconstructed fibers with the color mapped to different properties. While the color of the fiber is mapped to the normal at each point along the fiber in Figure 2(a), the derived uncertainty is mapped to the saturation of the color in Figure 2(b).

Uncertainty investigation widget. As mentioned in Section 3, the uncertainties from the wildbootstrap, the Bayesian tractography, and the PICo tractography are derived by resampling the diffusion tensor in

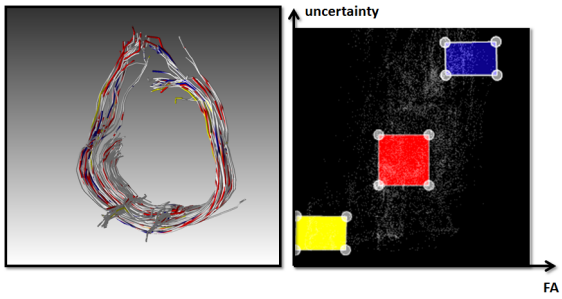

Fig. 3. Visual depiction of the relations between the FA and the derived uncertainty in PICo tractography. While the portions of fibers that have high FA, high uncertainty is colored blue, the portions with low FA, low uncertainty or average FA and average uncertainty are highlighted in yellow and red respectively.

each voxel of the input DTI data set. Therefore, there is an implicit relation between the distribution of the FA parameter obtained from the DTI, and the derived uncertainty on a per voxel basis. It turned out, that it is helpful to reveal this relation in the context of the reconstructed fibers to obtain an overview of the distribution of the derived uncertainty over the underlying FA. To this end we provide a 2D histogram view visualizing this relation. The image on the right in Figure 3 shows the 2D histogram representing the relation between FA and the derived uncertainty from the PICo approach. By placing colored primitives on this 2D histogram, the user can explore this relation. For instance, with the setup in Figure 3, the portions of the fibers that have a high FA and high uncertainty are highlighted in blue, while the portions with low FA values and low uncertainty or average FA and average uncertainty are highlighted in yellow and red respectively. Based on the result, the user can filter out for instance the fibers that have low FA and low certainty in the reconstructed fibers.

The proposed 2D histogram exploration widget can also be used to show the relation between different comparable derived uncertainties from the same DTI data set using different resampling techniques. This is helpful for the comparison of different resampling schemes as well as the comparison of a newly developed technique with the existing ones. The combination of visualization and interaction techniques realized in this system, has been applied to generate the results discussed in the next section.

5 Results and Discussions

In this Section, we present and discuss the results of the proposed uncertainty analysis and reduction technique applied to both synthetic and real-world data sets. In order to have a controlled setup, we first apply the proposed technique to a synthetic data set. We then apply the proposed technique to two real-world data sets: the monkey brain, and the human brain. In all cases we have applied the visual computing system described above, whereby the interaction time used for the uncertainty reduction was below five minutes.

5.1 Synthetic Data Set

For a controlled setup, we use the linear synthetic data set [40], which contains scans for 30 directions, each scan has the size of $150\times150\times16$ voxels, and a signal-to-noise ratio (SNR) of 30:1.

The FACT with wild bootstrap, and the Bayesian fiber tracking algorithms were applied to the data set to generate the initial sets of reconstructed fibers. The resampling scheme were set for 50 iterations, and the

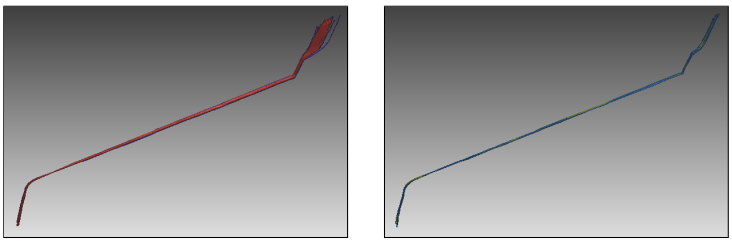

(a) (b)

Fig. 4. For illustration purposes, we have applied the proposed uncertainty analysis and reduction technique to a simple linear synthetic fiber dataset (courtesy of S. Deoni [40]). (*a*) is the visualization of a straight forward combination of the reconstructed fibers using different algorithms. (*b*) is the visualization of the output of the proposed uncertainty analysis and reduction technique applied to the same data sets.

Table 1. Result from the uncertainty derivation and reduction applied to the linear synthetic data set.

	FACT (Wild Bootstrap) tracking	Bayesian tracking	Uncertainty reduction
Number of fibers	50	50	28
Average uncertainty	0.244	0.130	0.11
Min uncertainty	0.347	0.000	0.000
Max uncertainty	0.700	1.000	0.396

seeding point was set on the original line. As a result, each fiber tracking algorithm produces a set of 50 reconstructed fibers. By applying the proposed uncertainty reduction method, we could achieve a new set of fibers, which contains whole fibers or the combination of portions of fibers with lower level uncertainty. The result is illustrated in Figure 4 and reflected quantitatively in Table 1. In addition to a lower average uncertainty level, the output of the uncertainty reduction technique also has a smaller range between the minimum and maximum uncertainty values. Moreover, the result is close to the original synthetic data.

5.2 Monkey Brain Data Set

In this test case, we use a DTI data set of the brain of a monkey, which contains scans of 30 directions, each scan has the size of $224\times224\times50$, and the voxel size is $2\times2\times2$mm. The resampling scheme in the fiber tracking algorithms were set to 50 iterations, and 12 seeding points were set in the middle of the corpus callosum. Table 2 shows the result of the uncertainty before and after applying the proposed technique. The proposed uncertainty reduction technique not only allows us to have a result with a lower average uncertainty level but also reduces the range between the minimum and maximum uncertainty.

5.3 Human Brain Data Set

For a more complex test case, we use the DTI data set from the VisContest 2010 which contains scans of 30 directions, each scan has the size of $128\times128\times72$, and the voxel size is $1.8\times1.8\times2.0$mm. The resampling scheme in the fiber tracking algorithms were also set to 50 iterations, and 12 seeding points were set in the middle of the corpus callosum. As can be seen in Table 3, the proposed approach for analyzing and reducing uncertainty improve the output. This is indicated by the fact that the average uncertainty decreases.

Table 2. Results from the uncertainty derivation and reduction applied to the monkey brain data set.

	Bayesian tracking	PICo tracking	Uncertainty reduction
Number of fibers	600	600	198
Average uncertainty	0.558	0.609	0.49
Min uncertainty	0.238	0.000	0.000
Max uncertainty	0.708	1.000	0.824

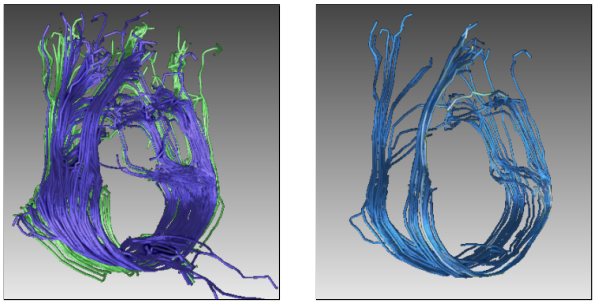

(a) (b)

Fig. 5. Visualization of a brute force combination of the reconstructed fibers from PICo and Bayesian tracking algorithms (*a*), and the result of the proposed uncertainty reduction technique (*b*).

Figure 5 illustrates the result of the proposed uncertainty reduction technique in comparison to a brute-force combination approach. While the brute-force combination of the reconstructed fibers from the PICo and Bayesian tractography does not yield a better result (see Figure 5(a)), the proposed technique enables a new set of fiber tracts with low level of uncertainty (Figure 5(b)).

It should be pointed out, that the reduction of the number of fibers does not result from discarding fibers, but from a combination of low uncertainty fibers. Having such a selection of lower uncertainty fibers can be beneficial for several applications. When for instance performing connectivity analysis, more reliable statements about the connectivity of regions can be made. As such connectivities influence the derivable functionality drastically, certainty is of high importance in this area.

6 Conclusions and Future Work

In this paper, we have proposed an novel approach for analyzing and reducing the uncertainty in reconstructed DTI fibers using different tracking algorithms. The uncertainty reduction is based on a unified uncertainty representation, which we derive from three deterministic and stochastic tractography algorithms:

Table 3. Results from the uncertainty derivation and reduction applied to the human brain data set.

	Bayesian tracking	PICo tracking	Uncertainty reduction
Number of fibers	300	300	87
Average uncertainty	0.506	0.701	0.39
Min uncertainty	0.036	0.000	0.000
Max uncertainty	0.69	1.000	0.65

FACT with wild bootstrapping, Bayesian tractography, and PICo tractography. Through this combination, it becomes possible to incorporate fiber uncertainty from different sources in order to generate new tractography results with reduced overall uncertainty. Therefore, we hope that this is one important step towards a wider acceptance of DTI techniques.

Although, by using the proposed technique, fiber tracts with reduced uncertainty can be generated, it would be interesting to integrate additional tractography algorithms on top of the three discussed approaches. We would further like to investigate if a biased uncertainty fusion would be beneficial in some cases. At the moment, the uncertainties obtained from the different algorithms are taken into account with equal weighting. However, for specific application cases or domain experts, it may be beneficial to apply a non-uniform weighting.

References

1. Moseley, M., Cohen, Y., Kucharczyk, J., Mintorovitch, J., Asgari, H., Wendland, M., Tsuruda, J., Norman, D.: Diffusion-weighted MR imaging of anisotropic water diffusion in cat central nervous system. Radiology **176** (1990) 439–445
2. Beaulieu, C.: The basis of anisotropic water diffusion in the nervous system – a technical review. NMR in Biomedicine **15** (2002) 435–455
3. Basser, P., Mattiello, J., Lebihan, D.: Estimation of the effective self-diffusion tensor from the {NMR} spin echo. Journal of Magnetic Resonance, Series B **103** (1994) 247 – 254
4. Ciccarelli, O., Catani, M., Johansen-Berg, H., Clark, C., Thompson, A.: Diffusion-based tractography in neurological disorders: concepts, applications, and future developments. The Lancet Neurology **7** (2008) 715–727
5. Basser, P., Pajevic, S., Pierpaoli, C., Duda, J., Aldroubi, A.: In vivo fiber tractography using DT-MRI data. Magnetic resonance in medicine **44** (2000) 625–632
6. Mori, S., van Zijl, P.: Fiber tracking: principles and strategies – a technical review. NMR in Biomedicine **15** (2002) 468–480
7. Lazar, M., Alexander, A.: Bootstrap white matter tractography (BOOT-TRAC). NeuroImage **24** (2005) 524–532
8. Liu, R.: Bootstrap procedures under some non-iid models. The Annals of Statistics (1988) 1696–1708
9. Whitcher, B., Tuch, D., Wisco, J., Sorensen, A., Wang, L.: Using the wild bootstrap to quantify uncertainty in diffusion tensor imaging. Human brain mapping **29** (2008) 346–362
10. Jones, D.: Tractography gone wild: Probabilistic fibre tracking using the wild bootstrap with diffusion tensor MRI. Medical Imaging, IEEE Transactions on **27** (2008) 1268–1274
11. Friman, O., Farneback, G., Westin, C.F.: A Bayesian approach for stochastic white matter tractography. Medical Imaging, IEEE Transactions on **25** (2006) 965–978
12. Parker, G., Haroon, H., Wheeler-Kingshott, C.: A framework for a streamline-based probabilistic index of connectivity (PICo) using a structural interpretation of MRI diffusion measurements. Journal of Magnetic Resonance Imaging **18** (2003) 242–254
13. Conturo, T.E., Lori, N.F., Cull, T.S., Akbudak, E., Snyder, A.Z., Shimony, J.S., McKinstry, R.C., Burton, H., Raichle, M.E.: Tracking neuronal fiber pathways in the living human brain. Proceedings of the National Academy of Sciences **96** (1999) 10422–10427
14. Mori, S., Crain, B., Chacko, V., Van Zijl, P.: Three-dimensional tracking of axonal projections in the brain by magnetic resonance imaging. Annals of neurology **45** (1999) 265–269
15. Weinstein, D., Kindlmann, G., Lundberg, E.: Tensorlines: advection-diffusion based propagation through diffusion tensor fields. In: Proceedings of the conference on Visualization '99: celebrating ten years. VIS '99, Los Alamitos, CA, USA, IEEE Computer Society Press (1999) 249–253
16. Kindlmann, G.: Superquadric tensor glyphs. In: Proceedings of the Sixth Joint Eurographics-IEEE TCVG conference on Visualization, Eurographics Association (2004) 147–154
17. Schultz, T., Kindlmann, G.: Superquadric glyphs for symmetric second-order tensors. Visualization and Computer Graphics, IEEE Transactions on **16** (2010) 1595–1604

18. Wittenbrink, C., Pang, A., Lodha, S.: Glyphs for visualizing uncertainty in vector fields. Visualization and Computer Graphics, IEEE Transactions on **2** (1996) 266–279
19. Merhof, D., Sonntag, M., Enders, F., Nimsky, C., Hastreiter, P., Greiner, G.: Streamline visualization of diffusion tensor data based on triangle strips. In Handels, H., Ehrhardt, J., Horsch, A., Meinzer, H.P., Tolxdorff, T., eds.: Bildverarbeitung fr die Medizin 2006. Informatik aktuell. Springer Berlin Heidelberg (2006) 271–275
20. Vilanova, A., Zhang, S., Kindlmann, G., Laidlaw, D.: An introduction to visualization of diffusion tensor imaging and its applications. In Weickert, J., Hagen, H., eds.: Visualization and Processing of Tensor Fields. Mathematics and Visualization. Springer Berlin Heidelberg (2006) 121–153
21. Enders, F., Sauber, N., Merhof, D., Hastreiter, P., Nimsky, C., Stamminger, M.: Visualization of white matter tracts with wrapped streamlines. In: Visualization, 2005. VIS 05. IEEE. (2005) 51–58
22. Chen, W., Zhang, S., Correia, S., Ebert, D.: Abstractive representation and exploration of hierarchically clustered diffusion tensor fiber tracts. Computer Graphics Forum **27** (2008) 1071–1078
23. Demiralp, C., Laidlaw, D.: Similarity coloring of DTI fiber tracts. In: Proceedings of DMFC Workshop at MICCAI. (2009)
24. Demiralp, C., Zhang, S., Tate, D., Correia, S., Laidlaw, D.H.: Connectivity-aware sectional visualization of 3D DTI volumes using perceptual flat-torus coloring and edge rendering. In: Proceedings of Eurographics. (2006)
25. Jianu, D., Zhou, W., gatay Demiralp, C., Laidlaw, D.: Visualizing spatial relations between 3D-DTI integral curves using texture patterns. Proceedings of IEEE Visualization Poster Compendium (2007)
26. Schultz, T., Theisel, H., Seidel, H.P.: Topological visualization of brain diffusion MRI data. Visualization and Computer Graphics, IEEE Transactions on **13** (2007) 1496–1503
27. Moberts, B., Vilanova, A., van Wijk, J.: Evaluation of fiber clustering methods for diffusion tensor imaging. In: Visualization, 2005. VIS 05. IEEE. (2005) 65–72
28. Lodha, S., Pang, A., Sheehan, R., Wittenbrink, C.: UFLOW: visualizing uncertainty in fluid flow. In: Visualization '96. Proceedings. (1996) 249–254
29. Chen, W., Ding, Z., Zhang, S., MacKay-Brandt, A., Correia, S., Qu, H., Crow, J., Tate, D., Yan, Z., Peng, Q.: A novel interface for interactive exploration of DTI fibers. Visualization and Computer Graphics, IEEE Transactions on **15** (2009) 1433–1440
30. Akers, D.: Cinch: a cooperatively designed marking interface for 3d pathway selection. In: Proceedings of the 19th annual ACM symposium on User interface software and technology. UIST '06, New York, NY, USA, ACM (2006) 33–42
31. Sherbondy, A., Akers, D., MacKenzie, R., Dougherty, R., Wandell, B.: Exploring connectivity of the brain's white matter with dynamic queries. Visualization and Computer Graphics, IEEE Transactions on **11** (2005) 419–430
32. Blaas, J., Botha, C., Peters, B., Vos, F., Post, F.: Fast and reproducible fiber bundle selection in DTI visualization. In: Visualization, 2005. VIS 05. IEEE. (2005) 59–64
33. Jianu, R., Demiralp, C., Laidlaw, D.: Exploring 3D DTI fiber tracts with linked 2D representations. Visualization and Computer Graphics, IEEE Transactions on **15** (2009) 1449–1456
34. Brecheisen, R., Vilanova, A., Platel, B., ter Haar Romeny, B.: Parameter sensitivity visualization for DTI fiber tracking. Visualization and Computer Graphics, IEEE Transactions on **15** (2009) 1441–1448
35. Seunarine, K., Cook, P., Embleton, K., Parker, G., Alexander, D.: A general framework for multiple-fibre PICo tractography. In: Medical Image Understanding and Analysis. (2006)
36. Zhu, T., Liu, X., Connelly, P., Zhong, J.: An optimized wild bootstrap method for evaluation of measurement uncertainties of DTI-derived parameters in human brain. Neuroimage **40** (2008) 1144–1156
37. Chung, S., Lu, Y., Henry, R.: Comparison of bootstrap approaches for estimation of uncertainties of DTI parameters. NeuroImage **33** (2006) 531–541
38. Vilanova, A., Berenschot, G., Van Pul, C.: DTI visualization with streamsurfaces and evenly-spaced volume seeding. In: Proceedings of the Sixth Joint Eurographics-IEEE TCVG conference on Visualization, Eurographics Association (2004) 173–182
39. Mallo, O., Peikert, R., Sigg, C., Sadlo, F.: Illuminated lines revisited. In: Visualization, 2005. VIS 05. IEEE. (2005) 19–26
40. Deoni, S.: PISTE - phantom images for simulating tractography errors. `http://neurology.iop.kcl.ac.uk/dtidataset/Common_DTI_Dataset.htm` (2008)